The transcription factor IbNAC29 positively regulates the carotenoid accumulation in sweet potato

Shihan Xing, Ruijie Li, Haoqiang Zhao, Hong Zhai, Shaozhen He, Huan Zhang, Yuanyuan Zhou, Ning Zhao, Shaopei Gao* and Qingchang Liu*

Key Laboratory of Sweet Potato Biology and Biotechnology, Ministry of Agriculture and Rural Affairs/Beijing Key Laboratory of Crop Genetic Improvement/Laboratory of Crop Heterosis and Utilization, Ministry of Education, College of Agronomy & Biotechnology, China Agricultural University, Beijing 100193, China

Email address of all authors

Shihan Xing (xingshihan@cau.edu.cn); Ruijie Li (liruijiestudent@126.com)
Haoqiang Zhao(zhaohaoqiang202209@163.com); Hong Zhai(zhaihong@cau.edu.cn)
Shaozhen He(sunnynba@cau.edu.cn); Huan Zhang(zhanghuan1111@cau.edu.cn)
Yuanyuan Zhou(zhou_yy_2020@163.com); Ning Zhao(zhaoning2012@cau.edu.cn)
Shaopei Gao (spgao@cau.edu.cn); Qingchang Liu (liuqc@cau.edu.cn)

*Correspondence: Qingchang Liu: Tel and fax +86 10 62733710, email liuqc@cau.edu.cn and Shaopei Gao: Tel +86 10 62732559, fax +86 10 62733710, email spgao@cau.edu.cn

Running title

IbNAC29 regulates carotenoid accumulation

Abstract

Carotenoid is a tetraterpene pigment beneficial for human health. Although the carotenoid biosynthesis pathway has been extensively studied in plants, relatively little is known about their regulation in sweet potato. Previously, we conducted the transcriptome database of differentially expressed genes between the sweet potato (*Ipomoea batatas*) cultivar “Weiduoli” and its high-carotenoid mutant "HVB-3". In this study, we selected one of these candidate genes, *IbNAC29*, for subsequent analyses. IbNAC29 belongs to the plant-specific NAC (NAM, ATAF1/2, and CUC2) transcription factor family. Relative *IbNAC29* mRNA level in the HVB-3 storage roots was ~1.71- fold higher than Weiduoli. Additional experiments showed that the contents of α-carotene, lutein, β-carotene, zeaxanthin, and capsanthin are obviously increased in the storage roots of transgenic sweet potato plants overexpressing *IbNAC29*. Moreover, the levels of carotenoid biosynthesis genes in transgenic plants were also up-regulated. Nevertheless, yeast one-hybrid assays indicated that IbNAC29 could not directly bind to the promoters of these carotenoid biosynthesis genes. Furthermore, the level of *IbSGR1* was down-regulated, whose homologous genes in tomato can negatively regulate carotene accumulation. Yeast three-hybrid analysis revealed that the IbNAC29-IbMYB1R1-IbAITR5 could form a regulatory module. Yeast one-hybrid, electrophoretic mobility shift assay, quantitative PCR analysis of chromatin immunoprecipitation and dual-luciferase reporter assay showed that IbAITR5 directly binds to and inhibits the promoter activity of *IbSGR1*, up-regulating carotenoid biosynthesis gene *IbPSY*. Taken together, *IbNAC29* is a potential candidate gene for the genetic improvement of nutritive value in sweet potato.

Introduction

Carotenoids are pigments, widely distributed in nature, and are divided into two groups: 1) carotenes including lycopene and α/β/γ-carotene, and 2) xanthophyll like lutein, zeaxanthin, and violaxanthin[1]. Over 750 natural carotenoids have been found in plants, algae, fungi, and bacteria[2,3]. Interestingly, carotenoids not only are crucial in these organisms that can synthesize them, but also in animals and humans. Humans must obtain carotenoids in their diet because their body cannot synthesize them[4,5].

In plants, carotenoids are biosynthesized via isopentenyl pyrophosphate (IPP) produced from the methylerythritol phosphate (MEP) pathway[6]. Phytoene synthase (PSY) is considered to be a major rate-limiting enzyme of carotenoid biosynthesis pathway. The subsequent cyclization of all-trans-lycopene by lycopene ε-cyclase (LCYE) and/or lycopene β-cyclase (LCYB) leads to the formation of symmetric orange β- and α-carotene in the β-β and β-ε branch, respectively. Then, ε-carotene hydroxylase (ECH) and β-carotene hydroxylase (BCH) add hydroxyl moieties to the cyclic end groups to produce lutein from α-carotene and zeaxanthin from β-carotene[7-9]. The epoxidation of zeaxanthin then produces antheraxanthin and violaxanthin[10], which are further converted by capsanthin-capsorubin synthase (CCS) into capsanthin and capsorubin, respectively[11,12]. Although the key enzymes involved in the carotenoid biosynthetic pathway have been extensively studied, the mechanism regulating carotenoid biosynthesis is still not well-explained.

The plant NAC (NAM, ATAF1/2, and CUC2) protein family is involved in diverse biological processes, including lateral root formation, secondary cell wall synthesis, and vegetative organ and fruit development[13,14]. Overexpression of *SlNAC1* decreases the levels of β-carotene, lycopene, and total carotenoid, while increasing the lutein content in tomato (*Solanum lycopersicum*)[14]. In *SlNAC4*-RNAi transgenic fruits, the total carotenoid level was significantly reduced after the break (B) stage[13,15]. Similarly, in the B+3 and B+10 stages of the NAC transcription factor *SlNAC3* mutant, *nor-like1*, carotenoid levels also significantly decreased[16]. On the

82 contrary, overexpression of *SlNAC-NOR* significantly accelerates the fruit ripening
83 process and produces higher carotenoid levels[17].
84 Besides, the MYB transcription factors also are important in regulating
85 carotenoid biosynthesis. Based on the number of MYB conserved domains, MYBs
86 are divided into (1) R1- (including one MYB domain), (2) R2R3- (including two MYB
87 domains), and (3) R1R2R3-type MYB (including three MYB domains) subgroups. At
88 present, mostly R2R3-type MYBs are reported to regulate carotenoid biosynthesis.
89 For example, overexpressing *AdMYB7* causes the accumulation of carotenoids and
90 chlorophyll in kiwifruit[18]. Conversely, downregulating the R2R3-MYB transcription
91 factor *RCP1* (*Reduced carotenoid pigmentation 1*) expression reduced carotenoid
92 content in *Mimulus lewisii* flowers[19]. Overexpression of *CrMYB68* (*Citrus reticulate*)
93 negatively regulates the expression of *NbBCH2* and *NbNCED5* to suppress the
94 transformation of α- and β-branch carotenoids in tobacco leaves[20]. Moreover, MYB
95 transcription factors form complexes with other proteins to participate in pigment
96 biosynthesis. In *Medicago truncatula*, the MtWP1-MtTT8-MtWD40-1 complex
97 regulates flower pigmentation via the anthocyanin and carotenoid biosynthesis[21].
98 According to previous studies, STAY-GREEN (SGR) is an evolutionarily
99 conserved chloroplast-targeted protein in higher plants which works in carotenoids
100 biosynthesis, chlorophyll degradation and senescence[22,23]. Silencing the *LeSGR1*
101 (*Lycopersicon esculentum*) expression inhibits chlorophyll degradation in the leaves
102 and fruits of tomato. Interestingly, SlSGR1 regulates lycopene and β-carotene
103 accumulation by interacting directly with SlPSY1, a key carotenoid biosynthesis
104 enzyme gene[24].
105 Sweet potato (*Ipomoea batatas* (L.) Lam. [$2n=B_1B_1B_2B_2B_2B_2 = 6x = 90$]) provides
106 carbohydrates and carotenoids for humans and is one of the most important food
107 crops across the world. Sweet potato, especially the orange-fleshed cultivars,
108 contains high levels of β-carotene, which could combat vitamin A deficiency[25,26]. In
109 this study, we found that overexpression (OE) of *IbNAC29* significantly increases the
110 carotenoid content. We also demonstrated that IbNAC29 participates in the

111 carotenoid biosynthesis by forming a regulatory module with IbMYB1R1 (R1-type
112 MYB) and IbAITR5. Moreover, IbAITR5 represses the transcription of *IbSGR1*. Our
113 results further indicated that IbNAC29 might enhance this repression, thus resulting
114 in the carotenoid accumulation.

115 **Results**

116 ***IbNAC29* is a potential candidate gene for regulating the carotenoid**
117 **biosynthesis pathway**

118 Previously, we performed RNA sequencing analyses on sweet potato cultivar
119 Weiduoli and its high-carotenoid mutant "HVB-3" (Fig. 1a) to identify the differentially
120 expressed genes[27]. Among these genes, the expressions of three NAC transcription
121 factor genes, including *IbNAC29*, *IbNAC74*, and *IbNAC87*, were upregulated in HVB-
122 3[27]. As shown in Fig. 1b, *IbNAC29* is homologous to the *NAC* transcription factor
123 *SlNOR-like1*. Regulation of carotenoid biosynthesis by *SlNOR-like1* in tomato has
124 been reported recently[16]. Furthermore, *IbNAC29* was widely expressed in the leaf,
125 stem, and root tissues of HVB-3 (Fig. 1c). Quantitative real-time PCR (qRT-PCR)
126 analysis showed mRNA level in the storage roots of HVB-3 was ~1.71- fold higher
127 than Weiduoli, thereby showing its potential link with carotenoid biosynthesis (Fig.
128 1d). Therefore, we selected *IbNAC29* for subsequent analyses.

129 The coding sequence of *IbNAC29* was 849 bp and contained three exons and
130 two introns, encoding a protein of 282 amino acids (Fig. 1e). Based on the NCBI's
131 Conserved Domains Database[28], N-terminal region of IbNAC29 contains a highly
132 conserved NAM DNA-binding domain (Fig. 1f).

133 **IbNAC29 is nuclear-localized and can function in transcriptional activation**

134 To further study the subcellular localization of IbNAC29, we expressed the IbNAC29-
135 GFP fusion protein in protoplasts. As a control, empty GFP plasmid was transfected
136 into protoplasts. As shown in Fig 2, GFP itself was distributed in the nucleus and the
137 cytoplasm as expected, whereas the fusion protein IbNAC29-GFP was nuclear-
138 localized (Fig. 2a). Furthermore, the position of green fluorescence from the

139 IbNAC29-GFP fusion protein merged with the red fluorescence from the nuclear
140 marker ARF1-mCherry[29], suggesting that IbNAC29 localizes to the nucleus.
141 Next, we used the transient expression system to investigate whether IbNAC29
142 acts as a transcriptional activator. We co-expressed the effector and reporter vectors
143 in protoplasts, and quantified the luciferase activity after 16 h incubation. The results
144 showed that the luciferase activity is significantly increased when IbNAC29 is co-
145 expressed (Fig. 2b), thus indicating that IbNAC29 is a transcriptional activator.

146 **Overexpression of *IbNAC29* enhances carotenoid levels in the storage roots of**
147 **sweet potato**

148 To further investigate whether *IbNAC29* regulates carotenoids in sweet potato, we
149 generated *IbNAC29*-OE plants by *Agrobacterium*-mediated transformation of sweet
150 potato variety Lizixiang (Supplemental Fig. S1 and S2). After examining the *IbNAC29*
151 mRNA levels in these plants using qRT-PCR, we selected three lines (OE-2, OE-7
152 and OE-23) with the up-regulated *IbNAC29* mRNA levels for further study
153 (Supplemental Fig. S1). Cross-sectional flesh samples of the transgenic lines were
154 slightly yellower and had orange spots relative to the wild type (WT) (Fig. 3a).
155 Since carotenoids are stored in plastids[30,31], we next analyzed the plastids in the
156 storage roots of transgenic *IbNAC29*-OE using transmission electron microscopy
157 (TEM). The number of carotenoid globules in the *IbNAC29*-OE plants was
158 significantly increased than in the WT (Fig. 3a), suggesting the high levels of
159 carotenoids accumulation in the storage roots of *IbNAC29*-OE plants.
160 Sweet potato contains various carotenoids, including α-carotene, lutein, β-
161 carotene, zeaxanthin, capsanthin, violaxanthin, β-cryptoxanthin, echinenone,
162 neoxanthin, antheraxanthin and capsorubin. Next, we determined the concentration
163 of different carotenoids in the storage roots of *IbNAC29*-OE and WT plants. We
164 found that the levels of α-carotene (0.0328-0.0403 μg/g DW), lutein (0.1816-0.2212
165 μg/g DW), β-carotene (0.1512-0.2888 μg/g DW), zeaxanthin (0.1081-0.1558 μg/g
166 DW), capsanthin (0.0082-0.0094 μg/g DW) and β-cryptoxanthin (0.8637-1.001 μg/g

167 DW) are significantly increased, respectively. While the levels of violaxanthin
168 (0.0023-0.0040 μg/g DW) is decreased in the *IbNAC29*-OE plants (Fig. 3b-l). There
169 is no significant difference in the level of capsorubin between IbNAC29-OE and WT
170 plants. Eventually, total carotenoid content is significantly increased in the storage
171 roots of transgenic plants compared with WT (Fig. 3m).

172 **Carotenoid biosynthesis-related genes are upregulated in *IbNAC29*-OE plants**

173 Next, we used qRT-PCR assays to determine the expression of carotenoid
174 biosynthesis-related genes in *IbNAC29*-OE plants and WT at storage root expansion
175 stage. The carotenoid biosynthesis pathway is shown in Fig. 4a. In this study, we
176 observed elevated mRNA levels of *IbDXS*, one MEP pathway gene (Fig. 4b) and four
177 carotene biosynthesis genes (*IbGGPPS*, *IbPSY*, *IbLCYE* and *IbLCYB*) (Fig. 4c-f).
178 Previous research has shown that CYP97A (Cytochrome P450 monooxygenase)
179 works synergistically with CYP97C to hydroxylate α-carotene into lutein[32-34]. Both
180 *IbCYP97A3* and *IbCYP97C1* are elevated in IbNAC29-OE. Therefore, the
181 upregulated *IbCYP97A3* and *IbCYP97C1* might lead to the lutein accumulation in
182 *IbNAC29*-OE plants (Fig. 3c and 4g-h).
183 Interestingly, we found increased zeaxanthin and capsanthin levels, but a
184 decreased violaxanthin level. The expression of *IbBCH*, *IbZEP* and *IbCCS* was also
185 activated in *IbNAC29*-OE. We thus proposed that the decreased violaxanthin level
186 may be because of its conversion to capsanthin under the high *IbCCS* expression
187 (Fig. 3e-g and 4i-k). Therefore, our results suggested that the upregulation of
188 carotenoid biosynthesis genes causes the carotenoid accumulation in the storage
189 roots of transgenic *IbNAC29*-OE sweet potato.

190 **IbNAC29 could not bind to the promoters of carotenoid biosynthesis-related**
191 **genes**

192 When *IbNAC29* was overexpressed in the sweet potato, the genes for carotenoid
193 biosynthesis were significantly elevated in *IbNAC29*-OE. Next, we performed yeast
194 one-hybrid (Y1H) experiment to investigated the potential relationship of IbNAC29

195 and the promoters of above genes . The promoter fragments of *IbGGPPS*, *IbPSY*,
196 *IbLCYE*, and *IbLCYB* were independently amplified by PCR using genomic DNA as
197 the template and cloned into the pLacZi2μ vector. The yeast activation domain (AD)
198 was fused with the coding sequence of *IbNAC29* to form the effector 42AD-IbNAC29
199 construct. Both the reporter constructs and the effector 42AD-IbNAC29 were
200 cotransformed into yeast. 42AD alone as a negative control. As shown in
201 Supplemental Fig. S4, IbNAC29 protein did not bind to these promoters. These
202 results remind us that IbNAC29 may indirectly influence carotenoid biosynthesis via
203 other factors.

204 **IbNAC29 forms a regulatory module with IbMYB1R1 and IbAITR5**

205 To investigate the possible interacting partners of IbNAC29 involved in carotenoid
206 biosynthesis, we screened the sweet potato yeast two-hybrid (Y2H) library. Among
207 these potential interacting proteins, we identified an R1-type MYB1 protein
208 IbMYB1R1. Previous studies have shown that R2R3-type MYB, along with other
209 factors, form a regulatory complex which affects anthocyanin biosynthesis[21,35,36].
210 Through yeast two-hybrid library screening, we isolated a IbMYB1R1-interacting
211 protein IbAITR5. IbAITR5 belongs to a novel family of transcription factors, working
212 as a member of ABA-induced transcription repressors (AITRs). The Y2H assays
213 revealed that although IbNAC29 and IbAITR5, individually interacted with IbMYB1R1,
214 there was no interaction between IbNAC29 and IbAITR5 (Fig. 5a). Using the yeast
215 three-hybrid (Y3H) assays, we also observed that IbNAC29, IbMYB1R1, and
216 IbAITR5 apparently formed a regulatory module (Fig. 5b). These interactions among
217 IbNAC29, IbMYB1R1, and IbAITR5 were verified in the leaf epidermal cells of
218 *Nicotiana benthamiana* using bimolecular fluorescence complementation (BiFC)
219 assays. We observed a sharp yellow fluorescence in the nucleus when IbNAC29-
220 nYFP or IbAITR5-nYFP was co-expressed with IbMYB1R1-cYFP, while negative
221 controls showed no YFP fluorescence signal (Fig. 5c). Furthermore, we found that
222 the IbMYB1R1 and IbAITR5 proteins were localized in the nuclei of the protoplasts

223 (Supplemental Fig. S5), which was consistent with the location of IbNAC29, thereby
224 suggesting that IbNAC29, IbMYB1R1, and IbMYB1R1 may form a regulatory module
225 and function in the nucleus.

226 Next, we used co-immunoprecipitation (co-IP) assays to investigate the
227 IbNAC29-IbMYB1R1 and IbMYB1R1-IbAITR5 interactions in vivo. We isolated the
228 total proteins co-expressed by IbMYB1R1-Myc with HA-IbNAC29 or HA-IbAITR5 in
229 the leaf epidermal cells of *Nicotiana benthamiana*, and incubated them with anti-c-
230 Myc agarose beads. We detected HA-IbNAC29 and HA-IbAITR5 in the
231 immunoprecipitated proteins, but not in the negative control (Fig. 5d-e). These
232 experiments further indicated that IbMYB1R1 physically interacts with IbNAC29 and
233 IbAITR5 in planta, confirming the previous results.

234 Taken together, these results confirmed that IbNAC29 could interact with
235 IbMYB1R1, which forms an intermediate bridge with IbAITR5 to potentially form the
236 IbNAC29-IbMYB1R1-IbAITR5 regulatory module.

237 **IbAITR5 directly binds to the *IbSGR1* promoter and represses its transcript**
238 **activity**

239 We first examined the relative mRNA level of the *SGR1*-homologous gene *IbSGR1* in
240 *IbNAC29*-OE plants using qRT-PCR. qRT-PCR analysis revealed that relative
241 *IbSGR1* mRNA level was strongly reduced in the *IbNAC29*-OE plants **(**Supplemental
242 Fig. **S6a)**, suggesting that *IbNAC29* may negatively regulate *IbSGR1*.

243 To test the hypothesis, we conducted Y1H assays to explore the relationship
244 between the IbNAC29-IbMYB1R1-IbAITR5 regulatory module and the *IbSGR1*
245 promoter. Interestingly, we found that IbAITR5, rather than IbNAC29 and IbMYB1R1,
246 directly binds to the *IbSGR1* promoter (Fig. 6a). Then, we used the dual-luciferase
247 reporter assays to assess the luciferase activity of *IbSGR1* driven by the IbAITR5.
248 These results revealed that when *IbSGR1pro:LUC* was co-transformed with IbAITR5,
249 IbAITR5 inhibited the *IbSGR1* promoter activity. Therefore, our data demonstrated
250 that IbAITR5 represses the *IbSGR1* promoter activity by binding to its promoter (Fig.

251 6b).

252 Next, we used the electrophoretic mobility shift assay (EMSA) and chromatin
253 immunoprecipitation-quantitative polymerase chain reaction (ChIP-qPCR) assays to
254 validate whether IbAITR5 could bind to the *IbSGR1* promoter. In the EMSA assay,
255 IbAITR5-GST bound to a 28 bp fragment of IbSGR1 *in vitro* (Fig. 6c). Additionally,
256 the ChIP-qPCR assays confirmed that IbAITR5 also binds in vivo to the *IbSGR1*
257 promoter (Fig. 6d). Thus, our results collectively suggested that IbAITR5 represses
258 *IbSGR1* transcription by directly binding to its promoter.

259 **IbNAC29-IbMYB1R1-IbAITR5 regulatory module regulates carotenoid**
260 **biosynthesis**

261 To further investigate how IbNAC29, IbMYB1R1, and IbAITR5 affected the
262 transcriptional activity of IbSGR1, we conducted the dual-luciferase reporter assays.
263 As shown in Fig. 7a, the luciferase activity remained unchanged when IbMYB1R1
264 vector co-transient with IbAITR5 and *IbSGR1pro* vectors compared with IbAITR5 and
265 *IbSGR1pro* vector co-transient in protoplasts. However, in the presence of
266 IbMYB1R1, IbNAC29 enhanced the inhibitory activity of IbAITR5 on the *IbSGR1*
267 promoter (Fig. 7a).

268 It has been reported that SlSGR1 influences the *SlPSY1* expression pattern in
269 tomato[24]. Furthermore, the dual-luciferase assays revealed that the IbSGR1 also
270 influences the expression of *IbPSY* (Fig. 7b). The repression of *IbPSY1* gene in the
271 in the presence of *IbSGR1* expression in accordance with previous studies[24].
272 Therefore, our results suggest that the IbNAC29-IbMYB1R1-IbAITR5 regulatory
273 module potentially regulates carotenoid biosynthesis via the regulation of *IbPSY1*.

274 **Discussion**

275 Carotenoids are tetraterpenoids molecules that play pivotal roles in photosynthesis,
276 pigmentation and development. Despite an in-depth mechanistic basis for
277 understanding the carotenoid biosynthesis, relatively little is known about how this
278 pathway is transcriptionally regulated. Previously, we conducted the transcriptome

279 database of differentially expressed genes between the Weiduoli and its high-
280 carotenoid mutant HVB-3[27]. Among these genes, NAC transcription factors *IbNAC29*,
281 *IbNAC74* and *IbNAC87* were upregulated in HVB-3. In this study，we selected and
282 characterized *IbNAC29* gene. Transgenic experiments demonstrated overexpression
283 of *IbNAC29* increased the levels of various carotenoids in the storage roots, including
284 α-carotene, lutein, β-carotene, zeaxanthin, and capsanthin (Fig. 3).
285 Indeed, the carotenoid biosynthetic gene expression (*IbDXS*, *IbGGPS*, *IbPSY,*
286 and etc) was also up-regulated in *IbNAC29* transgenic plants. This could potentially
287 explain why carotenoid accumulation is elevated. Previous reports have suggested
288 that overexpression of *PmDXS* and *IbGGPS* increased the carotenoid content in
289 *Arabidopsis*[37,38]. Furthermore, overexpressing *LCYE* elevates the carotenoid lutein
290 level in *Arabidopsis* leaves[39]. Also, overexpression of *IbLCYB2* increases the
291 carotenoid content in the sweet potato's storage roots[40]. In plants, the *SGR* gene
292 encodes the key enzyme for chlorophyll degradation[23]. In tomato, *SlSGR1* reportedly
293 regulates chlorophyll degradation[22,24]. Silencing *SlSGR1* inhibits chlorophyll
294 degradation, resulting in the retention of a green phenotype. As a matter of fact,
295 *SlSGR1* regulates the lycopene accumulation in tomato by directly inhibiting the
296 activity of a key carotenoid biosynthesis enzyme, SlPSY1[24]. Overexpression of
297 *CsPSY* enhances carotenoid accumulation in Hongkong kumquat [41]. Both CsSGRa
298 and CsSGRb interact with CsPSY1 to inhibit the citrus carotenoid biosynthesis,
299 chlorophyll degradation and carotenoid biosynthesis, which are highly conserved
300 processes in plants[42]. Similarly, the overexpression of *CsPSY* enhances carotenoid
301 accumulation in Hongkong kumquat[41]. Therefore, our result suggested that the
302 upregulation of carotenoid biosynthesis genes might cause the accumulation in the
303 carotenoids.
304 Previous studies have reported that the tomato NAC transcription factor SlNOR-
305 like1 directly binds to the *SGR1* promoter, thus regulating fruit ripening and
306 carotenoid accumulation[16]. However, Y1H assay indicated IbNAC29 could not
307 directly bind to the promoters of carotenoid biosynthesis-related enzymes. To explore

308 the possible mechanism of IbNAC29 involved in carotenoid biosynthesis, we
309 screened the sweet potato yeast two-hybrid (Y2H) library. Among these potential
310 interacting proteins, we identified an R1-type MYB1 protein IbMYB1R1. Previous
311 studies have shown that R2R3-type MYB, along with other factors, form a regulatory
312 complex which affects anthocyanin biosynthesis[21,35,36]. Through yeast two-hybrid
313 library screening, we isolated a IbMYB1R1-interacting protein IbAITR5. In our study,
314 the results showed that IbAITR5 could directly binds to the *IbSGR1* promoter,
315 inhibiting the expression of the *IbSGR1* (Fig. 6). The mRNA level of *IbSGR1* is down-
316 regulated in IbNAC29-OE, which is consistent with its negative role in carotenoid
317 accumulation. Although we detected enhanced carotenoids accumulation in the
318 *IbNAC29*-OE storage roots (Fig. 3), we did not find any direct interaction between
319 *IbNAC29* and the *IbSGR1* promoter (Fig. 6a). Therefore, our results suggested that
320 IbNAC29 might have a different regulatory mechanism with SlNOR-like1, possibly
321 because they belong to different clades in the evolutionary tree.
322 Through Y3H, EMSA, ChIP-qPCR and dual-luciferase assay analyses, our study
323 demonstrated that the IbNAC29-IbMYB1R1-IbAITR5 regulatory module mediates the
324 carotenoids biosynthesis via protein–protein interactions to regulate the downstream
325 target gene expression in sweet potato. It has been reported that AITRs are
326 transcription repressors in plants[43], and we found that the *IbAITR5* mRNA level in the
327 *IbNAC29*-OE plants was upregulated (Supplemental Fig. S6b). Thus, we proposed
328 that *IbNAC29* enhances the inhibitory activity of IbAITR5 by affecting its
329 transcriptional activity. This leads to reduce the expression of the *IbSGR1* (Fig. 2a
330 and 7a), resulting in further alleviation of the inhibition of IbSGR1 on mRNA level of
331 the key carotene biosynthesis gene *IbPSY*. Up-regulated expression of *IbPSY* might
332 lead to enhanced carotenoids accumulation in the storage roots (Fig. 8).
333 Altogether, our findings unveil the mechanism underlying the regulation of the
334 carotenoids accumulation and provide new insights for the genetic improvement in
335 the sweet potato. To further understand the mechanisms that regulate carotenoid
336 biosynthesis in staple crops, we will further identify the direct targets of *IbNAC29* by

337 combining transcriptome analysis with chromatin immunoprecipitation analysis in the
338 future. Moreover, we will attempt to use the CRISPR/Cas9-based gene editing
339 approach to further understand its role in the development of sweet potato.

340 **Materials and methods**

341 **Plant materials and growth conditions**

342 Sweet potato cultivar Weiduoli with orange-fleshed and its high carotenoid mutant
343 "HVB-3" were used for RNA sequencing analyses. Sweet potato cultivar Lizixiang
344 was used as the recipients for *Agrobacterium*-mediated transformation , which is a
345 pale-yellow flesh with low carotenoid content. Transgenic test-tube seedlings were
346 grown on Murashige and Skoog medium at 28 °C with 13-h-light/11-h-dark cycle. The
347 transgenic plants were cultivated in the field of the experimental stations of China
348 Agricultural University adhered to normal agricultural practice.

349 **Gene identification and sequence analysis**

350 Total RNA was extracted using TRIzol reagent (Invitrogen). Complementary DNAs
351 (cDNA) were obtained using HiFiScript gDNA Removal cDNA Synthesis Kit (CwBio)
352 according to the manufacturer's protocol. The RACE (rapid amplification of cDNA
353 ends) experiment was used to obtain the full-length cDNA sequence of *IbNAC29*.
354 According to the EST sequence obtained from previous studies[27], the coding
355 sequences of *IbMYB1R1, IbAITR5,* and *IbSGR1* were obtained from Lizixiang using
356 the homologous cloning method. DNAMAN software, MEGA 7.0 software, and the
357 Splign tool were used to analyze amino acid sequence alignments, exon-intron, and
358 phylogenetic relationships, respectively.

359 **Subcellular localization analysis**

360 The open reading frames of *IbNAC29*, *IbMYB1R1* and *IbAITR5* without the stop

361 codon were inserted into the pCAMBIA1300-35S-GFP vector. The recombinant
362 vector pBI121-ARF-mCherry containing a nuclear marker ARF1 was co-transformed
363 with pCAMBIA1300-35S-IbNAC29-GFP, pCAMBIA1300-35S-IbMYB1R1-GFP, and
364 pCAMBIA1300-35S-IbAITR5-GFP, respectively. Meanwhile, pCAMBIA1300-35S-GFP
365 and pBI121-35S-ARF1-mCherry were co-transformed into protoplasts as a control.
366 After growing for 16 h, the fluorescence signals of GFP and mCherry were visualized
367 by a confocal fluorescence microscopy (Olympus, Tokyo, Japan) under excitation
368 wavelengths of 488 nm and 546 nm, respectively.

369 **Sweet potato transformation and qRT-PCR analysis**

370 The embryogenic suspension cultures of Lizixiang were transformed with the
371 pCAMBIA1300-35S-IbNAC29-GFP vector via *Agrobacterium*-mediated
372 transformation[44]. The transgenic sweet potato plants were selected using hygromycin
373 as a selection marker. The plants were transferred to a greenhouse, planted in the
374 nutrient vegetative soil, and then transplanted to the field for phenotype observation.
375 The *IbActin* gene of sweet potato (*AY905538*) was used as the internal control for
376 expression analysis by qRT-PCR assays[45,46]. The mRNA levels of genes were
377 calculated by comparative CT method[47]. The experiment was conducted using three
378 biological replicates consisting of pools of three plants. Values are means ± SD of
379 three biological repeats.

380 **Measurement of carotenoid contents**

381 Carotenoids were extracted as described previously[37]. Three independent storage
382 roots from each freshly harvested WT and *IbNAC29*-OE transgenic plants were
383 mixed, respectively. Carotenoids and the relative contents were measured as
384 previously described[48].

385 **Transmission electron microscope (TEM)**

386 The storage roots of *IbNAC29*-OE and WT were fixed as previously described[40]. The
387 number of carotenoid globules was observed using TEM (JEM-1230, Tokyo, Japan).

388 **Yeast assays**

389 In the Y1H assay, the open reading frames of *IbNAC29*, *IbMYB1R1*, and *IbAITR5*
390 sequences were separately cloned into the pB42AD vector. The promoter sequences
391 of *IbGGPPS*, *IbPSY*, *IbLCYB*, *IbLCYE*, and *IbSGR1* genes from Lizixiang were
392 cloned separately into the pLacZi2μ vector. In short, various LacZ reporter plasmids
393 were cotransformed with the pB42AD fusion constructs into EGY48 yeast strain. The
394 pLacZi2μ reporter and pB42AD were co-transformed as negative controls.
395 Transformants were grown on SD/-Trp-Ura dropout plates containing 5-bromo-4-
396 chloro-3-indolyl-β-D-galactopyranoside (X-Gal) for blue color development.

397 Y2H assay was done according to the Matchmaker™ Gold Yeast Two-Hybrid
398 System User Manual (Clontech). The coding sequences of *IbNAC29*, *IbMYB1R1*,
399 and *IbAITR5* were cloned into either the bait vector pGBKT7 or the prey vector
400 pGADT7. Transformed Y2H-Gold yeast cells were patched onto the SD/-Leu/-Trp
401 and SD/-Leu/-Trp/-His/-Ade +6 mM 3AT plates and grown at 30°C.

402 Y3H assay was conducted as previously described[49]. The open reading frames
403 of *IbNAC29* and *IbMYB1R1* were cloned into the pBridge vector, while the coding
404 sequence of *IbAITR5* was cloned into the pGADT7 vector. The combinations of
405 pBridge-IbNAC29-IbMYB1R1 with pGADT7-IbAITR5, pBridge-IbNAC29-IbMYB1R1
406 with pGADT7, and pBridge with pGADT7-IbAITR5 were co-transformed into yeast.
407 The combinations containing the empty pBridge or pGADT7 vectors were used as
408 negative controls. Transformed Y2H-Gold yeast cells were patched on the SD/-Leu/-
409 Trp and SD/-Leu/-Trp/-His/-Met +6 mM 3AT plates and grown at 30°C.

410 **BiFC assay**

411 Empty pSPYNE-35S or the pSPYCE-35S vector cloned with the *IbNAC29*,
412 *IbMYB1R1*, and *IbAITR5* coding sequences were transformed into the *Agrobacterium*
413 *tumefaciens* strain EHA105. Combinations of pSPYNE and pSPYCE vectors,
414 together with P19, were infiltrated into the *Nicotiana benthamiana* leaf epidermal
415 cells. The YFP signal was observed by using a laser confocal scanning microscope
416 at an excitation wavelength of 488 nm after 48 h growth (Olympus, Tokyo, Japan).

417 **Co-IP assay**

418 Co-IP assay was performed as mentioned previously[46]. The anti-HA primary antibody
419 (MilliporeSigma), anti-Myc primary antibody (MilliporeSigma), Goat anti-mouse IgG
420 secondary antibody (Light chain specific, Easybio), and Anti-c-Myc agarose beads
421 (MilliporeSigma) were used to detect samples.

422 **Dual-luciferase assay**

423 Rice shoot protoplasts were isolated and used for the dual-luciferase assays, as
424 described previously[50]. For the transcriptional activity assay, the empty pBD vector
425 was used as the negative control to measure the transcriptional activity of *IbNAC29*.
426 For the DNA-promoter interaction assay, the *IbNAC29*, *IbMYB1R1*, *IbAITR5,* and
427 *IbSGR1* coding sequences were cloned separately into the pGreenII 62-SK vector.
428 The *IbSGR1* and *IbPSY* promoters were cloned separately into the pGreenII0800-
429 LUC vector. Firefly luciferase (LUC) and Renilla luciferase (REN) activity levels were
430 measured using a dual-luciferase reporter assay system (Promega, USA). Four
431 technical replicates were conducted in the experiments.

432 **EMSA**

433 EMSA was performed according to the manufacturer's instructions (Thermo Fisher
434 Scientific, USA). Glutathione beads purified recombinant GST-labeled IbAITR5

protein expressed in *E. coli* Transetta (DE3). The NACRS element containing biotin-labeled probes synthesized by Tsingke (Beijing) were used as binding probes, while unlabeled probes were used as competing probes.

ChIP-qPCR analysis

The ChIP assay was carried out as described previously[46]. The plants of pSuper1300-IbAITR5-GFP were cut into pieces and immediately fixed with 1% (v/v) formaldehyde solution. Next, the samples were ground into fine powders under liquid nitrogen. StepOnePlus™ was used to analyze the enrichment of immunoprecipitated DNA. *IbSGR1* promoter P2 fragment contained a NACRS element (sequence is ACGTGA), while P1 having no NACRS element served as the negative control. Four technical replicates were conducted in the experiments using. All the above primer sequences are shown in Supplemental Table S1.

Data availability statements

The data supporting the findings of this work are available within the paper and its Supplementary Information.

Accession numbers

Sequence data from this article can be found in the Sweet Potato Genomics Resource database (http://sweetpotato.uga.edu) under accession numbers *IbNAC29* (itf01g25900.t1), *IbSGR1* (itf08g00520.t1), *IbMYB1R1* (itf03g18010.t1), *IbAITR5* (itf11g06190.t1), *IbGGPPS* (itf08g03960.t1), *IbPSY* (itf03g05110.t1), *IbLCYE* (itf12g20540.t1), and *IbLCYB* (itf01g24560.t1).

Acknowledgements

This study was supported by the National Natural Science Foundation of China (31872878) and the earmarked fund for CARS-10-Sweetpotato.

459 **Author contributions**

460 S.X. and Q.L. designed the experiments. S.X., R.L., H.Zhao, H.Zhai, H. Zhang, H.S.,
461 Y.Z., and N.Z. performed the experiments. S.X., R.L., Y.Z. and S.G. analyzed the
462 data. S.X. drafted the manuscript. S.G. and Q.L. revised and finalized the
463 manuscript. All authors discussed the results and approved the final article.

464 **Conflict of interests**

465 The authors declare no competing financial interests.
466

467 **Supplementary data**

468 **Supplemental Figure S1** Generation of the *IbNAC29*-OE plants.
469 **Supplemental Figure S2** Identification of *IbNAC29*-OE plants by PCR.
470 **Supplemental Figure S3** qRT-PCR analysis of *IbNAC29* mRNA levels in the
471 leaves of the transgenic sweet potato plants.
472 **Supplemental Figure S4** Y1H assay showed that 42AD-IbNAC29 did not
473 activate the expression of the *LacZ* reporter genes driven by *IbGGPPS*,
474 *IbPSY*, *IbLCYE,* and *IbLCYB* promoters in yeast cells.
475 **Supplemental Figure S5** Subcellular localization of IbMYB1R1 and IbAITR5
476 in rice protoplasts.
477 **Supplemental Figure S6** Transcript levels of *IbSGR1* (a) and *IbAITR5* (b) in
478 *IbNAC29*-OE storage roots.

479 **References**

480 1. McQuinn, R.P. *et al.* Manipulation of ZDS in tomato exposes
481 carotenoid–and ABA–specific effects on fruit development and ripening.
482 *Plant Biotechnol. J* **18**, 2210-2224 (2020).
483 2. Johnson, J.D. Do carotenoids serve as transmembrane radical

484 channels? *Free Radical Bio. Med.* **47**, 321-323 (2009).
485 3. Nisar, N., Li, L., Lu, S., Khin, N.C. & Pogson, B.J. Carotenoid
486 metabolism in plants. *Mol. Plant* **8**, 68-82 (2015).
487 4. Krinsky, N.I. & Johnson, E.J. Carotenoid actions and their relation to
488 health and disease. *Mol. Aspects Med.* **26**, 459-516 (2005).
489 5. Fraser, P.D. & Bramley, P.M. The biosynthesis and nutritional uses of
490 carotenoids. *Prog. Lipid. Res.* **43**, 228-265 (2004).
491 6. Pulido, P., Toledo-Ortiz, G., Phillips, M.A., Wright, L.P. & Rodríguez-
492 Concepción, M. Arabidopsis J-protein J20 delivers the first enzyme of
493 the plastidial isoprenoid pathway to protein quality control. *Plant Cell*
494 **25**, 4183-4194 (2013).
495 7. Cazzonelli, C.I. & Pogson, B.J. Source to sink: regulation of carotenoid
496 biosynthesis in plants. *Trends Plant Sci.* **15**, 266-274 (2010).
497 8. Farré, G. *et al.* Travel advice on the road to carotenoids in plants. *Plant*
498 *Sci.* **179**, 28-48 (2010).
499 9. Kang, L. *et al.* Metabolic engineering of carotenoids in transgenic
500 sweetpotato. *Breed. Sci.* **67**, 27-34 (2017).
501 10. Ku, H.-K. *et al.* Alteration of carotenoid metabolic machinery by β-
502 carotene biofortification in rice grains. *J. Plant Biol.* **62**, 451-462 (2019).
503 11. Jeknić, Z. *et al.* Cloning and functional characterization of a gene for
504 capsanthin-capsorubin synthase from tiger lily (*Lilium lancifolium*
505 Thunb.'Splendens'). *Plant Cell Physiol.* **53**, 1899-1912 (2012).
506 12. Guzman, I., Hamby, S., Romero, J., Bosland, P.W. & O'Connell, M.A.
507 Variability of carotenoid biosynthesis in orange colored *Capsicum spp*.
508 *Plant Sci.* **179**, 49-59 (2010).
509 13. Kou, X. *et al.* SNAC4 and SNAC9 transcription factors show
510 contrasting effects on tomato carotenoids biosynthesis and softening.
511 *Postharvest Biol. Tec.* **144**, 9-19 (2018).
512 14. Ma, N. *et al.* Overexpression of tomato *SlNAC1* transcription factor

513 alters fruit pigmentation and softening. *BMC Plant Biology* **14**, 1-14
514 (2014).
515 15. Zhu, M. *et al.* A new tomato NAC (NAM/ATAF1/2/CUC2) transcription
516 factor, SlNAC4, functions as a positive regulator of fruit ripening and
517 carotenoid accumulation. *Plant Cell Physiol.* **55**, 119-135 (2014).
518 16. Gao, Y. *et al.* A NAC transcription factor, NOR-like1, is a new positive
519 regulator of tomato fruit ripening. *Hortic. Res.* **5**, 75 (2018).
520 17. Gao, Y. *et al.* Re-evaluation of the nor mutation and the role of the
521 NAC-NOR transcription factor in tomato fruit ripening. *J. Exp. Bot.* **71**,
522 3560-3574 (2020).
523 18. Aharoni, A. *et al.* The strawberry FaMYB1 transcription factor
524 suppresses anthocyanin and flavonol accumulation in transgenic
525 tobacco. *Plant J.* **28**, 319-332 (2001).
526 19. Sagawa, J.M. *et al.* An R2R3−MYB transcription factor regulates
527 carotenoid pigmentation in *Mimulus lewisii* flowers. *New Phytol.* **209**,
528 1049-1057 (2016).
529 20. Zhu, F. *et al.* An R2R3−MYB transcription factor represses the
530 transformation of α− and β−branch carotenoids by negatively
531 regulating expression of *CrBCH2* and *CrNCED5* in flavedo of *Citrus*
532 *reticulate*. *New Phytol.* **216**, 178-192 (2017).
533 21. Meng, Y. *et al.* The MYB activator WHITE PETAL1 associates with
534 MtTT8 and MtWD40-1 to regulate carotenoid-derived flower
535 pigmentation in *Medicago truncatula*. *Plant Cell* **31**, 2751-2767 (2019).
536 22. Hörtensteiner, S. Stay-green regulates chlorophyll and chlorophyll-
537 binding protein degradation during senescence. *Trends Plant Sci.* **14**,
538 155-162 (2009).
539 23. Thomas, H. & Howarth, C.J. Five ways to stay green. *J. Exp. Bot.* **51**,
540 329-337 (2000).
541 24. Luo, Z. *et al.* A STAY−GREEN protein SlSGR1 regulates lycopene and

542 β - carotene accumulation by interacting directly with SlPSY1 during
543 ripening processes in tomato. *New Phytol.* **198**, 442-452 (2013).
544 25. Xiao, Y., Zhu, M. & Gao, S. Genetic and genomic research on sweet
545 potato for sustainable food and nutritional security. *Genes* **13**, 1833
546 (2022).
547 26. Teow, C.C. *et al.* Antioxidant activities, phenolic and β-carotene
548 contents of sweet potato genotypes with varying flesh colours. *Food*
549 *Chem.* **103**, 829-838 (2007).
550 27. Li, R. *et al.* De novo transcriptome sequencing of the orange-fleshed
551 sweet potato and analysis of differentially expressed genes related to
552 carotenoid biosynthesis. *Int. J. Genomics* **2015**, 843802 (2015).
553 28. Marchler-Bauer, A. *et al.* CDD: NCBI's conserved domain database.
554 *Nucleic Acids Res.* **43**, D222-D226 (2015).
555 29. Waller, F., Furuya, M. & Nick, P. OsARF1, an auxin response factor
556 from rice, is auxin-regulated and classifies as a primary auxin
557 responsive gene. *Plant Mol. Biol.* **50**, 415-425 (2002).
558 30. Li, L. & Yuan, H. Chromoplast biogenesis and carotenoid accumulation.
559 *Arch. Biochem. Biophys.* **539**, 102-109 (2013).
560 31. Vishnevetsky, M., Ovadis, M. & Vainstein, A. Carotenoid sequestration
561 in plants: the role of carotenoid-associated proteins. *Trends Plant Sci.*
562 **4**, 232-235 (1999).
563 32. Li, X., Sun, J., Chen, Z., Jiang, J. & Jackson, A. Metabolite profile and
564 genes/proteins expression in β-citraturin biosynthesis during fruit
565 ripening in Chinese raspberry (*Rubus chingii* Hu). *Plant Physiol. Bioch.*
566 **163**, 76-86 (2021).
567 33. Liang, M.-H., Xie, H., Chen, H.-H., Liang, Z.-C. & Jiang, J.-G.
568 Functional identification of two types of carotene hydroxylases from the
569 green alga Dunaliella bardawil rich in lutein. *ACS Synth. Biol.* **9**, 1246-
570 1253 (2020).

571 34. Quinlan, R.F. *et al.* Synergistic interactions between carotene ring
572 hydroxylases drive lutein formation in plant carotenoid biosynthesis.
573 *Plant Physiol.* **160**, 204-214 (2012).
574 35. An, J.-P. *et al.* Dynamic regulation of anthocyanin biosynthesis at
575 different light intensities by the BT2-TCP46-MYB1 module in apple. *J.*
576 *Exp. Bot.* **71**, 3094-3109 (2020).
577 36. Nuraini, L. *et al.* Anthocyanin regulatory and structural genes
578 associated with violet flower color of *Matthiola incana*. *Planta* **251**, 1-15
579 (2020).
580 37. Chen, W. *et al.* A sweetpotato geranylgeranyl pyrophosphate synthase
581 gene, *IbGGPS*, increases carotenoid content and enhances osmotic
582 stress tolerance in *Arabidopsis thaliana*. *PLoS One* **10**, e0137623
583 (2015).
584 38. Li, R. *et al.* Characterization and function of the 1-deoxy-D-xylose-5-
585 phosphate synthase (DXS) gene related to terpenoid synthesis in
586 Pinus massoniana. *Int. J. Mol. Sci.* **22**, 848 (2021).
587 39. Cunningham Jr, F.X. *et al.* Functional analysis of the beta and epsilon
588 lycopene cyclase enzymes of Arabidopsis reveals a mechanism for
589 control of cyclic carotenoid formation. *Plant Cell* **8**, 1613-1626 (1996).
590 40. Kang, C. *et al.* A lycopene β-cyclase gene, *IbLCYB2*, enhances
591 carotenoid contents and abiotic stress tolerance in transgenic
592 sweetpotato. *Plant Sci.* **272**, 243-254 (2018).
593 41. Zhang, J. *et al.* Functional characterization of Citrus PSY gene in
594 Hongkong kumquat (*Fortunella hindsii* Swingle). *Plant Cell Reports* **28**,
595 1737-1746 (2009).
596 42. Zhu, K. *et al.* Regulation of carotenoid and chlorophyll pools in
597 hesperidia, anatomically unique fruits found only in Citrus. *Plant*
598 *Physiol.* **187**, 829-845 (2021).
599 43. Tian, H. *et al.* A novel family of transcription factors conserved in

600 angiosperms is required for ABA signalling. *Plant Cell Environ.* **40**,
601 2958-2971 (2017).
602 44. Yu, B. *et al.* Efficient Agrobacterium tumefaciens-mediated
603 transformation using embryogenic suspension cultures in sweetpotato,
604 *Ipomoea batatas* (L.) Lam. *Plant Cell Tiss. Organ Cult.* **90**, 265-273
605 (2007).
606 45. Zhang, H. *et al.* A non–tandem CCCH–type zinc–finger protein,
607 IbC3H18, functions as a nuclear transcriptional activator and enhances
608 abiotic stress tolerance in sweet potato. *New Phytol.* **223**, 1918-1936
609 (2019).
610 46. Zhang, H. *et al.* IbBBX24 promotes the jasmonic acid pathway and
611 enhances fusarium wilt resistance in sweet potato. *Plant Cell* **32**, 1102-
612 1123 (2020).
613 47. Schmittgen, T.D. & Livak, K.J. Analyzing real-time PCR data by the
614 comparative CT method. *Nat. Protoc.* **3**, 1101-1108 (2008).
615 48. Li, R. *et al.* A ζ-carotene desaturase gene, *IbZDS*, increases β-carotene
616 and lutein contents and enhances salt tolerance in transgenic
617 sweetpotato. *Plant Sci.* **262**, 39-51 (2017).
618 49. Ma, Y.-N. *et al.* Jasmonate promotes artemisinin biosynthesis by
619 activating the TCP14-ORA complex in *Artemisia annua*. *Sci. Adv.* **4**,
620 eaas9357 (2018).
621 50. Hellens, R.P. *et al.* Transient expression vectors for functional
622 genomics, quantification of promoter activity and RNA silencing in
623 plants. *Plant Methods* **1**, 1-14 (2005).
624
625

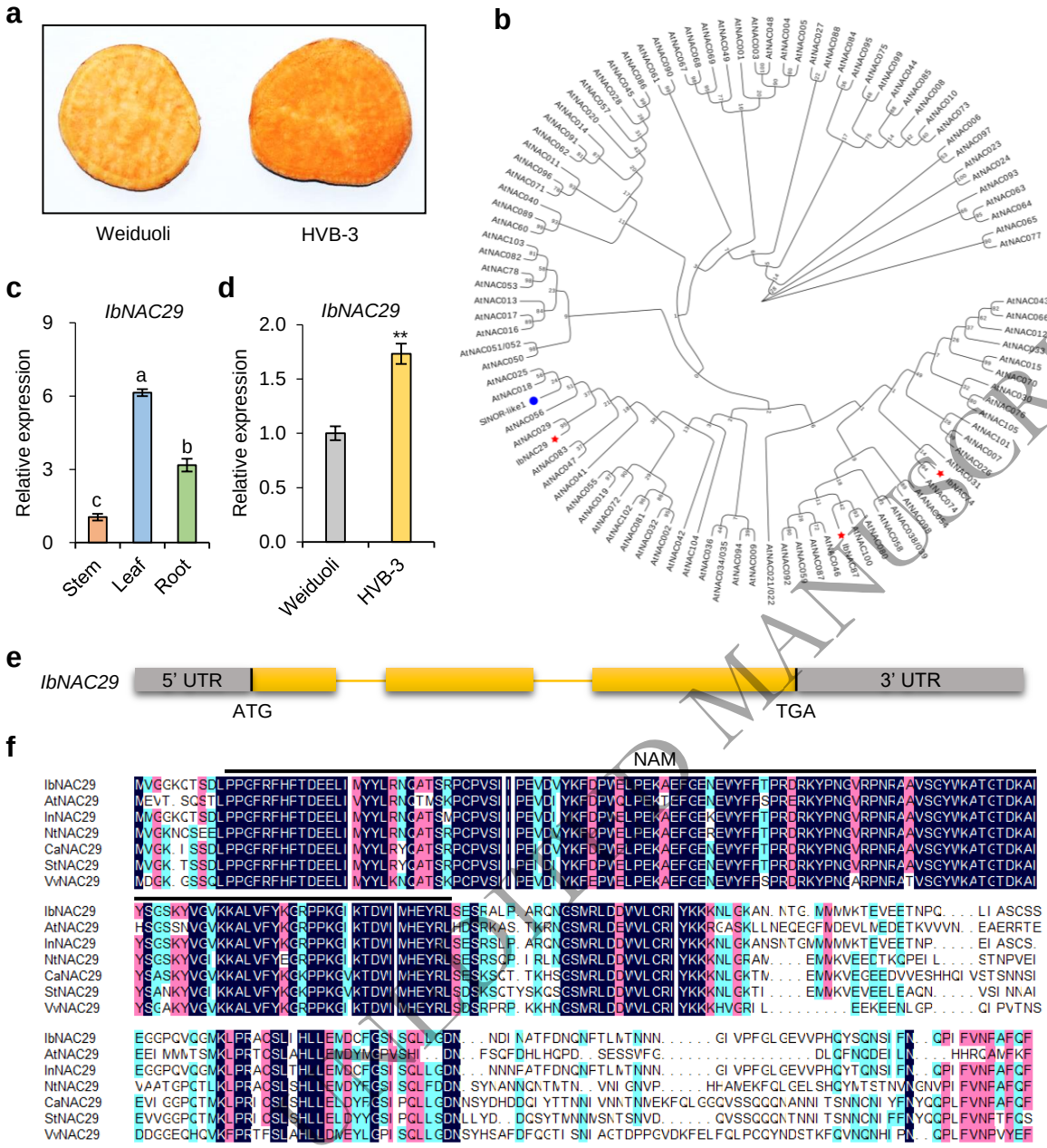

Figure 1. Molecular characterization of IbNAC29. **a** Phenotype of orange-fleshed sweet potato cultivar Weiduoli and its mutant HVB-3 with high carotenoid content. **b** Phylogenetic analysis of the NAC protein in *Arabidopsis* and sweet potato (IbNAC29, IbNAC74, IbNAC87) was performed with 1000 bootstrap iterations using the neighbor-joining method in MEGA 7.0. The numbers on the tree nodes represent 1000 repeated boot values. IbNAC29, IbNAC74, and IbNAC87 from carotenoid-related transcriptome data are marked with red stars. SlNOR-like1, a reported *NAC* transcription factor linked to carotenoid biosynthesis in tomato, is marked with a blue circle. **c** Relative mRNA level of *IbNAC29* in different tissues of 4-week-old in vitro–grown HVB-3 plants. *IbActin* was used as the internal control. **d** Relative mRNA level of *IbNAC29* in the storage roots of Weiduoli and HVB-3 at storage root expansion stage. *IbActin* was used as the internal control. Error bars indicate SD (n = 3). **indicates $P < 0.01$, respectively, by Student's *t*-test. **e** Gene structure analyses of *IbNAC29*. Grey boxes indicate the untranslated region, including 5' untranslated regions (UTRs) and 3' UTR. Yellow boxes and lines represent exons and introns, respectively. **f** Multiple sequence alignment of NAC29 from different species. Plant species include *Arabidopsis thaliana* (At), *Ipomoea nil* (In), *Nicotiana tabacum* (Nt), *Capsicum annuum* (Ca), *Solanum tuberosum* (St) and *Vitis vinifera* (Vv). The NAM domain is represented by black lines.

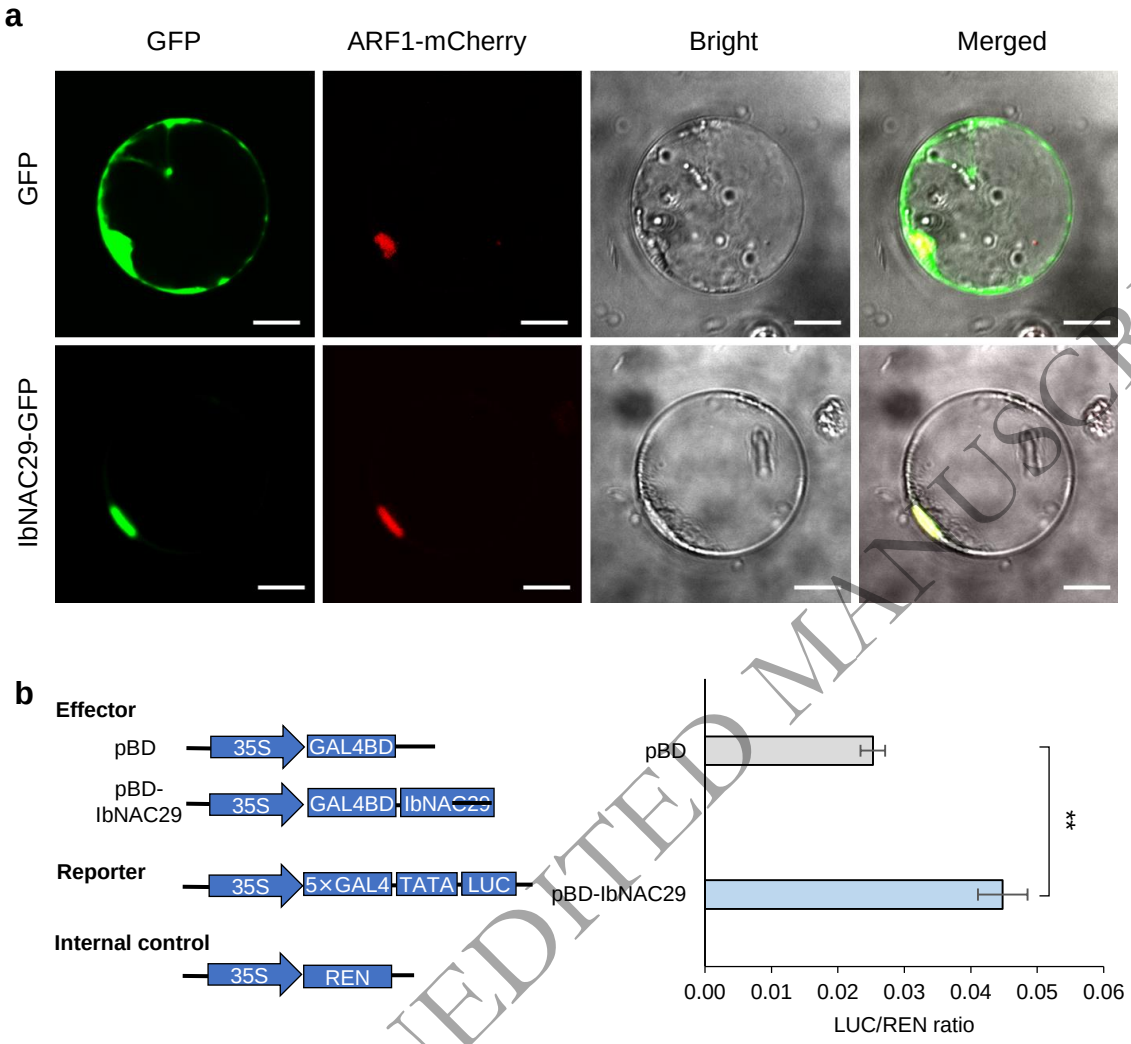

Figure 2 Subcellular localization and transcriptional activity of IbNAC29. **a** Subcellular localization of IbNAC29 in protoplasts. IbNAC29-GFP was co-transformed with ARF1-mCherry, which was used as a nuclear marker. Bar = 10 μm. **b** Transactivation assay of IbNAC29 in protoplasts. The GAL4 BD empty vector was used as a negative control. The expression level of REN was used as an internal control. Error bars indicate SD (n = 3). ** indicates a significant difference from that of pBD at $P < 0.01$, by Student's *t*-test.

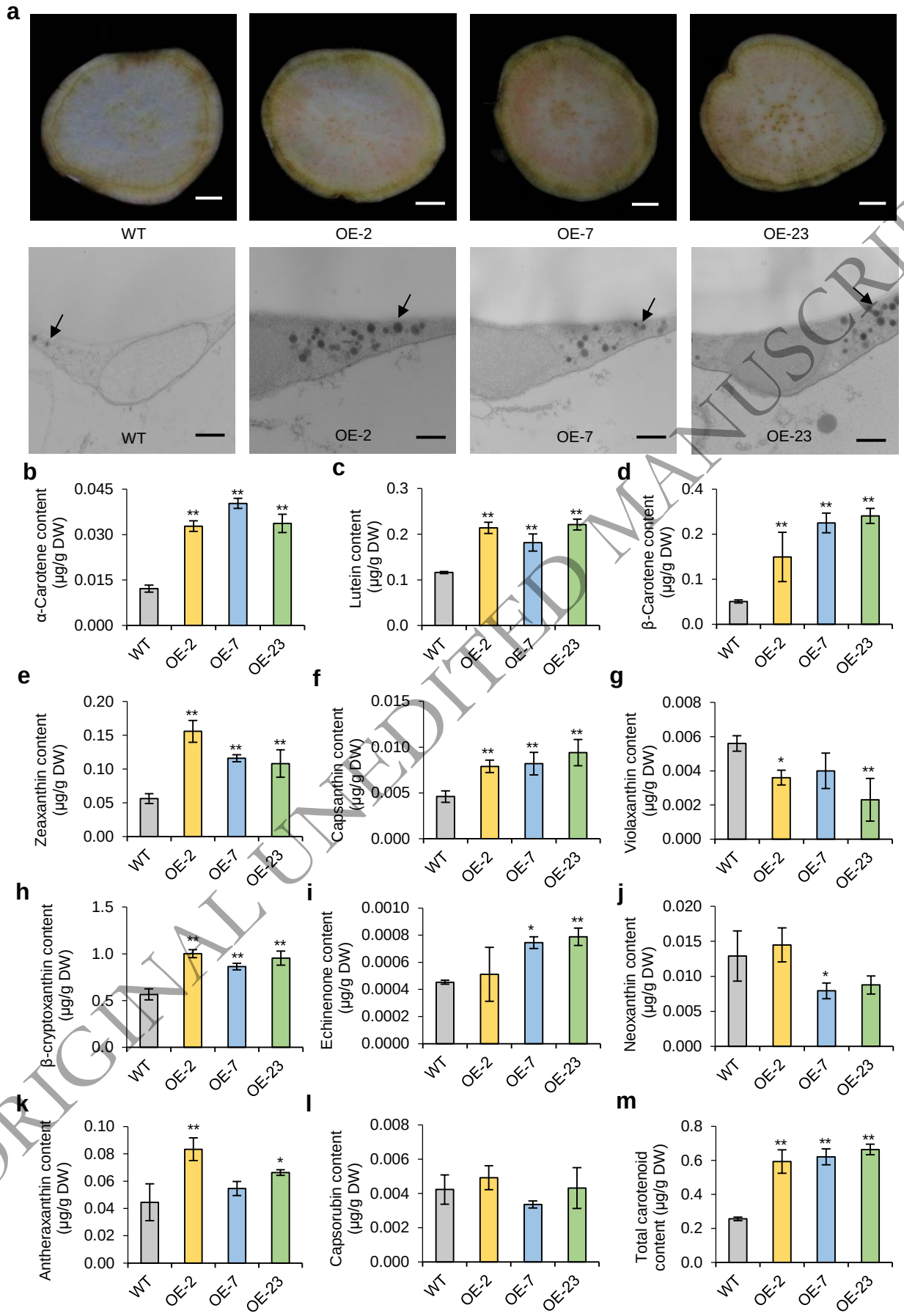

Figure 3 Overexpression of *IbNAC29* increases the carotenoid content in the storage roots of sweet potato during the maturity stages. **a** Storage roots' transverse sections (up), Bar = 1 cm; The carotenoid globules (dark grey) are shown in the electron microscopy images (down), Bar = 500 nm. Arrows indicate the carotenoid globules. **b-l** Levels of α-carotene, lutein, β-carotene, zeaxanthin, capsanthin, violaxanthin, β-cryptoxanthin, echinenone, neoxanthin, antheraxanthin, and capsorubin in the storage roots of WT and transgenic plants, respectively. m Total carotenoid content of WT and transgenic plants. Error bars indicate SD (n = 3). * and ** indicate a significant difference from that of WT at $P < 0.05$ and $P < 0.01$, respectively, by Student's *t*-test.

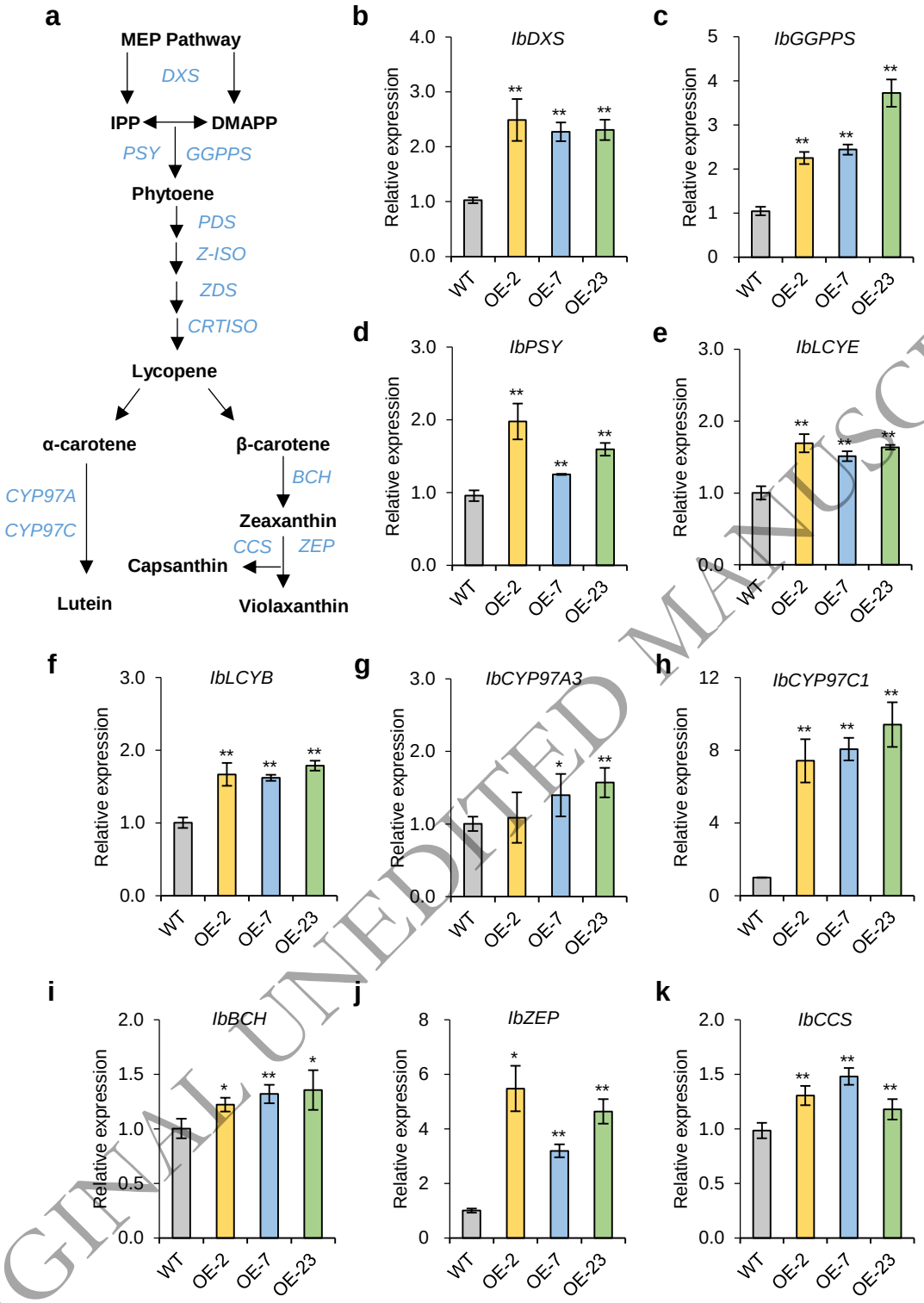

Figure 4 Carotenoid biosynthetic pathway and expression levels of carotenoid biosynthetic-related genes in the storage roots of *IbNAC29*-OE plants. **a** General carotenoid biosynthetic pathway in plants. **b** MEP pathway gene, *IbDXS,* for carotenoid precursor supply. **c-f** Carotene biosynthetic genes, including *IbGGPPS*, *IbPSY*, *IbLCYE* and *IbLCYB*. **g-k** Xanthophyll biosynthetic genes, including *IbCYP97A3*, *IbCYP97C1*, *IbBCH*, *IbZEP* and *IbCCS*. *IbActin* was used as the internal control. The transcript level in WT was set as control. Error bars indicate SD (n = 3). * and ** indicate a significant difference from that of WT at $P < 0.05$ and $P < 0.01$, respectively, by Student's *t*-test.

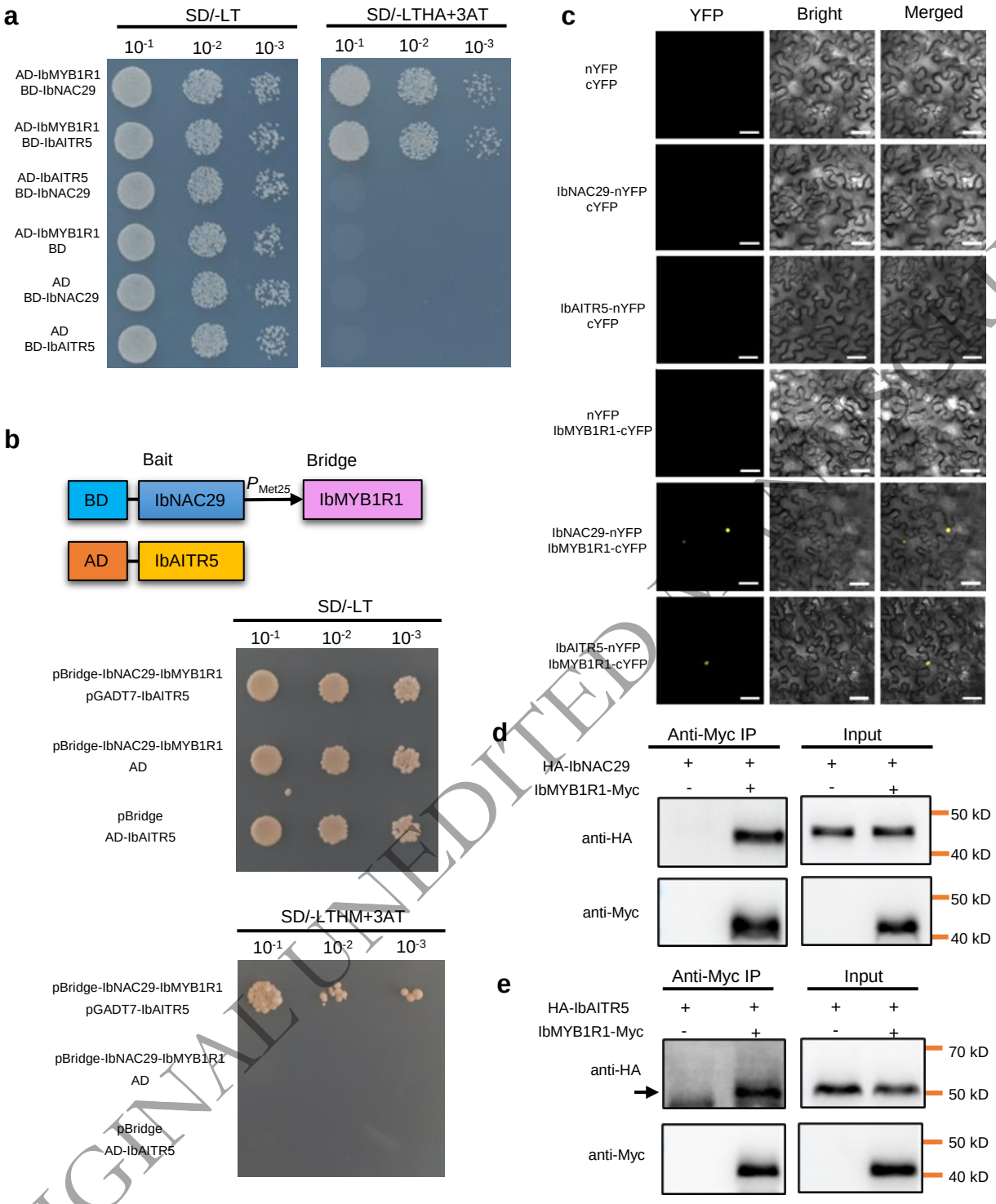

Figure 5 Interactions between IbNAC29, IbMYB1R1, and IbAITR5. **a** Interactions among IbNAC29, IbMYB1R1 and IbAITR5 by Y2H assays. **b** Y3H assays detected the interactions between IbNAC29, IbMYB1R1, and IbAITR5. **c** Confirmation of the interaction between IbNAC29 and IbMYB1R1, IbMYB1R1 and IbAITR5 by BiFC, as indicated by the yellow fluorescent signal. Bar = 50 μm. **d** and **e** co-IP assays showing that IbMYB1R1 interacts with IbNAC29 (**d**) and IbAITR5 (**e**) in vivo. Total proteins from *Nicotiana benthamiana* leaf cells expressing IbMYB1R1-Myc, HA-IbNC29 and HA-IbAITR5 were extracted and incubated with anti-Myc magnetic beads. Total extracts before (input) and after IP were detected with anti-HA and anti-Myc antibodies.

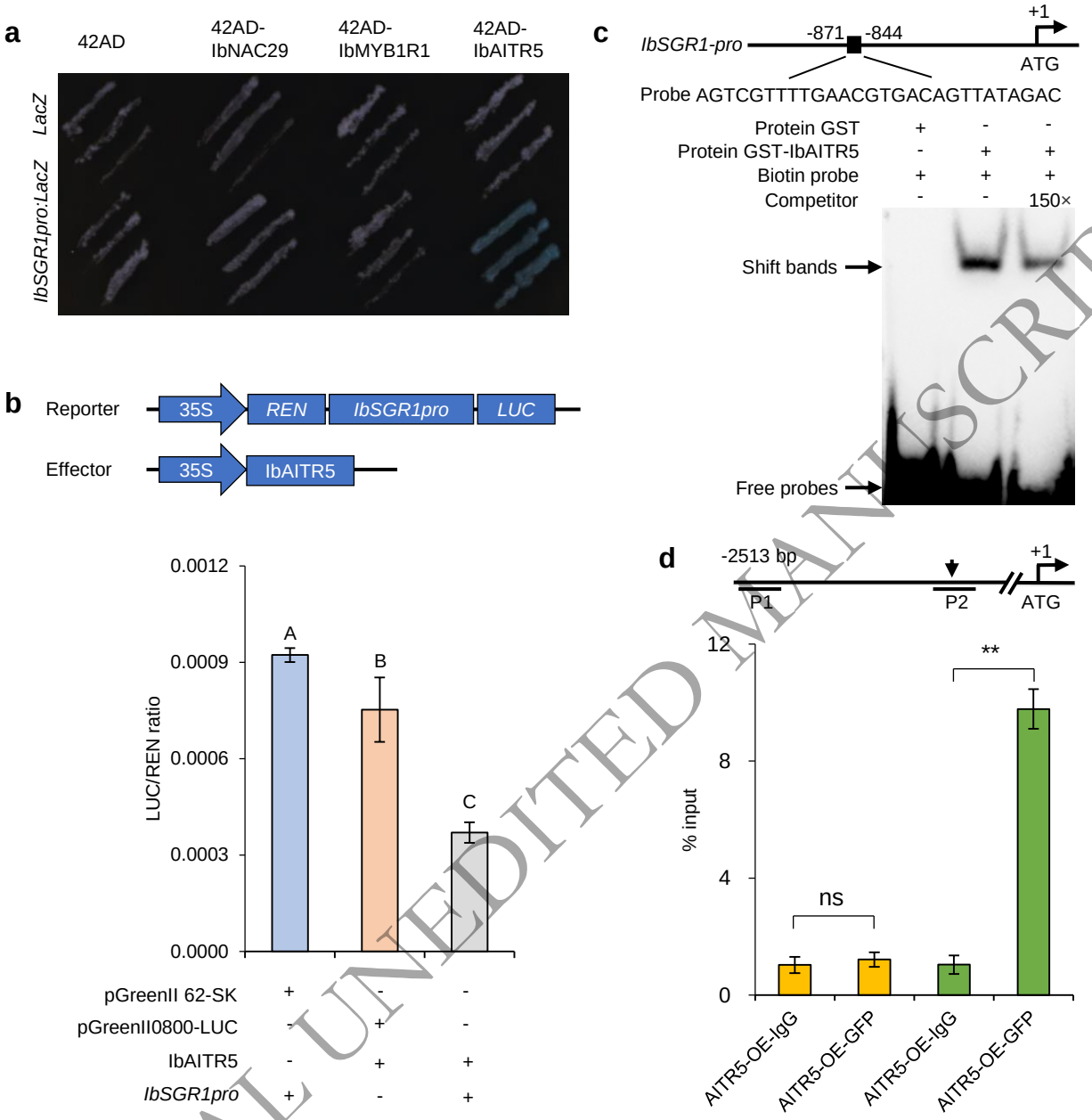

Figure 6 Interactions of IbAITR5 with the *IbSGR1* promoter. **a** Y1H assay showing that IbAITR5 binds to the promoter of *IbSGR1*. Yeast cells containing *IbSGR1pro:LacZ* were transformed with IbNAC29, IbMYB1R1 and IbAITR5 fused with the 42AD and grown on medium containing X-Gal. Coexpression of 42AD/LacZ, 42AD- IbNAC29/LacZ, 42AD- IbMYB1R1/LacZ, 42AD-IbAITR5/LacZ, and 42AD/*IbSGR1pro:LacZ* was used as the negative controls. **b** IbAITR5 inhibited the promoter activity of *IbSGR1* determined by the dual-luciferase assays in protoplasts. Relative activity of the *IbSGR1* promoter was represented by the LUC/REN ratio. "+" and "–" indicated presence and absence, respectively. Error bars indicate SD (n = 4). Ordinary one-way ANOVA multiple comparison, with different letters indicating the statistically significant differences at $P < 0.01$. **c** EMSA showing that IbAITR5 binds to an NACRS element of the *IbSGR1* promoter. The recombinant IbAITR5-GST protein retarded the shift of the labelled probes; 150× indicated adding excess non-labelled probes as competitors. "+" and "–" indicated presence and absence, respectively. **d** ChIP-qPCR analysis showed IbAITR5 could bind to the *IbSGR1* promoter in the chromatin immunoprecipitated with an anti-GFP antibody from the 35S:IbAITR5-GFP plants. AITR5-OE-IgG, no antibody control samples. The NACRS element in segment P2 was represented by an arrow. Segment P1 was used as the negative control. Error bars indicate SD (n = 4). ns, no significance. ** indicates $P < 0.01$, as determined by Student's t-test analysis.

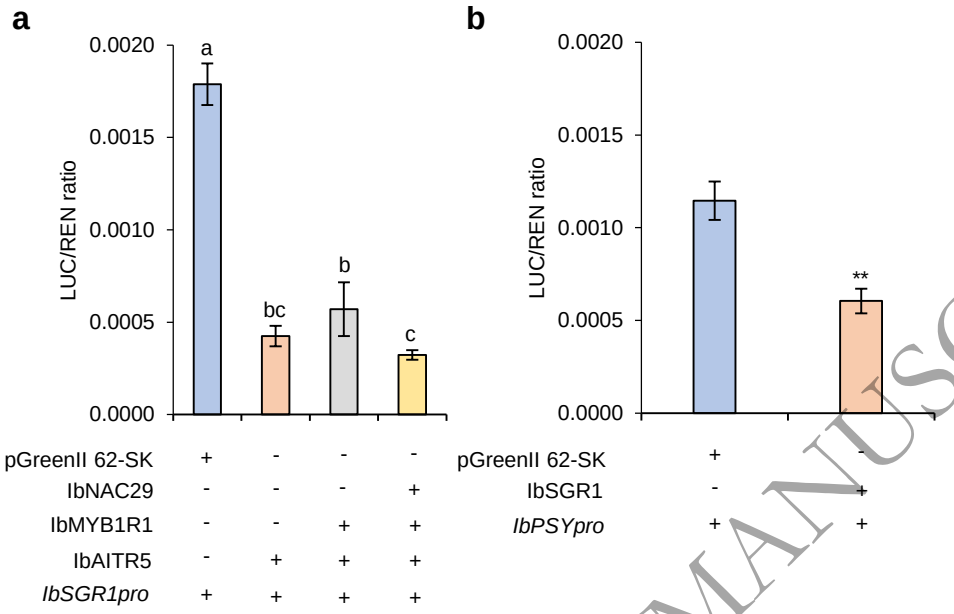

Figure 7 Effects of IbNAC29, IbMYB1R1, and IbAITR5 and their complexes on downstream genes. **a** IbNAC29 enhanced the inhibitory activity of IbAITR5 on the downstream *IbSGR1pro* via IbMYB1R1 in the protoplasts. "+" and "−" indicated presence and absence, respectively. Error bars indicate SD (n = 4). Ordinary one-way ANOVA multiple comparison, with different letters indicating the statistically significant differences at $p < 0.05$. **b** IbSGR1 inhibited the *IbPSY* promoter activity in protoplasts. "+" and "−" indicated presence and absence, respectively. Error bars indicate SD (n = 4). Ordinary one-way ANOVA multiple comparison, with different letters indicating statistically significant differences at $p < 0.01$.

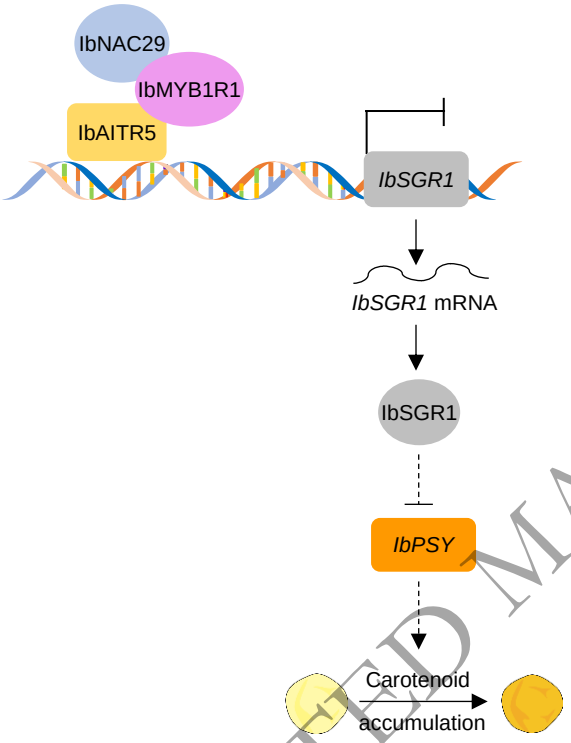

Figure 8 Proposed model of how *IbNAC29* regulates carotenoid biosynthesis. IbNAC29, IbMYB1R1, and IbAITR5 form a regulatory module. IbAITR5 binds to and represses the promoter activity of *IbSGR1*. Elevated levels of *IbNAC29* enhance the IbAITR5-mediated inhibition of IbSGR1 activity, reducing the inhibition of *IbPSY* gene expression and increasing the accumulation of carotenoids.